LncRNA CASC2 regulates high glucose-induced proliferation, extracellular matrix accumulation and oxidative stress of human mesangial cells *via* miR-133b/FOXP1 axis

X.-L. ZHANG¹, H.-Q. ZHU², Y. ZHANG³, C.-Y. ZHANG⁴, J.-S. JIAO⁵, X.-Y. XING¹

Xuelian Zhang and Haiqing Zhu contributed equally to this work

Abstract. – OBJECTIVE: Diabetic nephropathy (DN) is one of the primary complications of diabetes. Long non-coding RNA cancer susceptibility candidate 2 (CASC2) has been established to function in DN, while its role in high glucose (HG)-induced human mesangial cells (HMCs) remains limited.

MATERIALS AND METHODS: The expression level of CASC2 and miR-133b was detected by quantitative real-time polymerase chain reaction (qRT-PCR). Cell proliferation was assessed using cell counting kit-8 (CCK-8) assay. Extracellular matrix (ECM) accumulation was monitored through the expression levels of collagen IV (Col IV) and fibronectin (FN) using qRT-PCR and western blot analyses. Oxidative stress was observed through the expression of NADPH oxidase2 (NOX2) and the activity of malondialdehyde (MDA) and superoxide dismutase (SOD) using western blot or corresponding detection kit. The expression of forkhead box P1 (FOXP1) at mRNA and protein levels was determined by qRT-PCR and Western blot, respectively. The relationship between miR-133b and CASC2 or FOXP1 was predicted by online bioinformatics tools and verified by dual-luciferase reporter assay or RNA pull-down.

RESULTS: The expression of CASC2 was reduced in serum from DN patients and HG-induced HMCs. CASC2 upregulation inhibited HG-induced HMCs proliferation, ECM accumulation and oxidative stress. MiR-133b was a target of CASC2 with a high level in serum from DN patients and HG-induced HMCs, and its enrichment reversed the effects of CASC2 upregulation. Besides, FOXP1 was a target of miR-133b with a low level in HG-induced HMCs, and its knockdown abolished the impacts of CASC2 upregulation.

CONCLUSIONS: CASC2 upregulation suppressed HG-induced proliferation, ECM accumulation and oxidative stress of HMCs through miR-133b /FOXP1 regulatory axis, suggesting that CASC2 was a novel biomarker for DN treatment.

Key Words:

CASC2, MiR-133b, FOXP1, Diabetic nephropathy, High glucose.

Introduction

Diabetes is a chronic disease of metabolic disorders with long-term hyperglycemia¹. Diabetic nephropathy (DN) is a common complication of diabetes and is characterized by progressive deterioration of kidney function². DN is the leading cause of death associated with cardiovascular disease and the end-stage renal failure³. Numerous factors closely related to DN progression have been reported, such as inflammation, oxidative stress, activated hexose, renal extracellular matrix (ECM)accumulation and polyol pathways4. Available evidence suggests that high-glucose (HG) is the major cause of DN, leading to the stimulative oxidative stress and inflammation in mesangial cells (MC)^{5,6}. Although a variety of therapeutic strategies have been developed to prevent the development of DN, the therapeutic effect is generally weak with prognostic adverse effects^{7,8}. Therefore, it is urgent to develop novel therapeutic targets to improve the treatment of DN.

¹Department of Endocrinology, China-Japan Friendship Hospital, Beijing, China

²Department of Endocrinology, Emergency General Hospital, China

³Department of Endocrinology, Affiliated Hospital of Hebei University, Hebei, China

⁴Statistical Teaching and Research Department, China-Japan Friendship Hospital, Beijing, China

⁵Department of Neurology, China-Japan Friendship Hospital, Beijing, China

Long non-coding RNAs (lncRNAs) are a subgroup of non-coding RNAs with over 200 nucleotides in length. It was well established that numerous lncRNAs were implicated in the pathological processes of DN. For example, IncRNA PVT1 was highly expressed in HMCs with HG stimulation, and it contributed to the expression of ECM proteins, such as collagen IV (Col IV), fibronectin (FN) and TGF-β1, suggesting that PVT1 regulated the development of DN through modulating the accumulation of ECM9,10. LncRNA MALAT1 was abnormally up-regulated in the early stage of DN, and it accelerated the inflammation response and oxidative stress¹¹. While lncRNA TUG1 was poorly expressed in the podocytes of diabetic mice, and it ameliorated the progression of DN through the regulation of MCs proliferation, cell cycle and ECM enrichment ^{12,13}. LncRNA cancer susceptibility candidate 2(CASC2) was depicted to play diverse roles in the development of human cancers¹⁴⁻¹⁶, and the low expression of CASC2 in serum and renal tissues of diabetes patients was also mentioned¹⁷. However, the potential role of CASC2 in HMCs induced by HG has not been explored.

It is well known that lncRNAs exert their roles by acting as sponges of downstream microRNAs (miRNAs). MiRNAs are a cluster of non-coding RNAs containing approximately 22 nucleotides¹⁸. Dozens of miRNAs were identified to be aberrantly regulated in DN¹⁹, including miR-133b²⁰. Accumulating studies have proved that miR-133b participated in several human diseases, such as Alzheimer's disease, atrial dilatation and diverse cancers²¹⁻²³. Unfortunately, the function of miR-133b in HG-induced HMCs is lacking and needs further exploration. Generally, miRNAs function in the regulation of gene expression via interacting with the 3' untranslated region (3' UTR) of downstream mRNAs, conducing to transcript degradation and translation inhibition ²⁴. Forkhead box P1 (FOXP1) belongs to FOX family proteins. Up to now, FOXP1 was widely investigated in the regulation of biological processes, including hepatic glucose homeostasis, inflammation response and tumorigenesis²⁵⁻²⁷. Interestingly, the role of FOXP1 in glomerular mesangial cells exposed to HG was partly stated²⁸. Nevertheless, the action mechanism of FOXP1 in DN is inadequate.

Currently in this study, the expression of CASC2 in the serum of DN patients and HG-induced HMCs was detected, and the gain-function experiments were performed to ensure the role of CASC2 in HG-induced HMCs. In addition,

the downstream targets of CASC2 were identified to reveal the underlying action mechanism. The purpose of this study was to explore a novel action mechanism of CASC2 and a promising therapeutic strategy in DN.

Materials and Methods

Serum Samples Collection

A total of 62 DN patients and 50 healthy volunteers were recruited from China-Japan Friendship Hospital. Their blood samples were collected and centrifuged at 2000 × g to obtain serum samples. All serum samples were frozen in liquid nitrogen and stored at -80°C before use. Each patient or volunteer had signed informed consent. This study was approved by the Ethics Committee of China-Japan Friendship Hospital.

Cell Culture and HG Treatment

Human mesangial cells (HMCs) were purchased from BeNa Culture Collection (Suzhou, China) and maintained in 90% Dulbecco's Modified Eagle's Medium (DMEM; Sigma-Aldrich, St. Louis, MO, USA) containing 10% fetal bovine serum (FBS; Sigma-Aldrich, St. Louis, MO, USA) at 37°C with 5% CO₂. For HG treatment, HMCs were exposed to 90% DMEM and 10% fetal bovine serum (FBS) containing 30 mM glucose (HG), or 5.5 mM glucose (Control). Treated cells were incubated for 24 h and used for the following experiments.

Cell Transfection

CASC2 was amplified and constructed onto pcDNA 3.1 vector for CASC2 overexpression, named as CASC2, and empty pcDNA3.1 vector (vector) was served as control. MiR-133b mimics (miR-133b), miR-133b inhibitors (anti-miR-133b) and their negative controls (miR-NC and anti-NC) were purchased from Ribobio (Guangzhou, China). Small interference RNA against FOXP1 (si-FOXP1) and its negative control (si-NC) were assembled by Genepharma (Shanghai, China). All items were introduced into HMCs with or without HG treatment using Lipofectamine 2000 (Invitrogen, Carlsbad, CA, USA) in line with the manufacturer's instruction.

Quantitative Real-Time Polymerase Chain Reaction (qRT-PCR)

Total RNA was extracted from serum samples and HMCs using TRIzol Reagent (Invitrogen), and

complementary DNA (cDNA) was synthesized using TagMan Reverse Transcription Reagents (Invitrogen) or using MicroRNA Reverse Transcription Kit (Applied Biosystems, Foster City, CA, USA). Fast SYBR Green Master Mix (Applied Biosystems) was used for qRT-PCR analysis under BioRad CFX96™ (Bio-Rad, Hercules, CA, USA). The expression levels were normalized by β-actin and small nuclear RNA U6 and calculated by the $2^{-\Delta\Delta Ct}$ method. The primers used were listed as below: CASC2, forward (F): 5'-GCA-CATTGGACGGTGTTTCC-3' and reverse (R): 5'-CCCAGTCCTTCACAGGTCAC-3'; FOX-5'-TCAGTGGTAACCCTTCCCTTA-3' P1.F: 5'-GTACAGGATGCACGGCTTG-3'; and Col-IV,F: 5'-CACAGCCAGACCATTCAG-3' and R: 5'-AAGCGTTTGCGTAGTAATTG-3'; FN,F: 5'-AGAGTGGAAGTGTGAGAG-3' and R: 5'-TTGTAGGTGAATGGTAAGAC-3'; β-actin, 5'-ATGGGTCAGAAGGATTCCTATGTG-3' and R: 5'-CTTCATGAGGTAGTCAGTCAG-GTC-3';miR-133b,F: 5'-GAACCAAGCCGC-CCGAGA-3' and R: 5'-CCGCCCTGCTGTGCT-GGT-3'; U6,F: 5'-CTCGCTTCGGCAGCACA-3' and R: 5'-AACGCTTCACGAATTTGCGT-3'.

Cell Counting Kit-8 (CCK-8) Assay

HMCs with different transfection were planted into 96-well plates (5×10^3 cells per well). Then 10 μ L CCK-8 solution (Beyotime, Shanghai, China) was added into each well at the indicated time points (24 h, 48 h and 72 h) for another 4 h at 37°C. Afterwards, the absorbance was measured at 450 nm using the Multiskan Ascent (Thermo Fisher Scientific, Waltham, MA, USA).

Western Blot

HMCs were incubated with RIPA buffer (Beyotime, Beijing, China) to acquire total protein. The concentrations of protein samples were measured using the BCA Protein kit (Beyotime). Then, the equal protein was separated by 10% sodium dodecyl sulfate-polyacrylamide gel electrophoresis (SDS-PAGE) and electro-transferred onto polyvinylidene difluoride (PVDF) (Bio-Rad Hercules, CA, USA) membranes. Subsequently, the membranes were immersed in 5% skim milk for 1.5 h and probed with the primary antibodies against Col-IV (1:1000, ab6586; Abcam, Cambridge, MA, USA), FN (1:1000, ab2413; Abcam), NOX2 (1:1000, ab80508; Abcam), FOXP1 (1:5000, ab16645; Abcam), and β-actin (1:5000, ab8227; Abcam) overnight at 4°C. Afterwards, the membranes were incubated with horseradish peroxidase (HRP)-conjugated secondary antibodies (1:5000, ab205718; Abcam). The indicated proteins were emerged using enhanced chemiluminescent (ECL) kit (Thermo Fisher Scientific, Waltham, MA, USA).

Detection of Malondialdehyde (MDA) and Superoxide Dismutase (SOD) Release

To ascertain the activity of MDA and SOD, the release of MDA and SOD was ascertained using Lipid Peroxidation MDA Assay Kit (Beyotime) and Total Superoxide Dismutase Assay Kit (Beyotime), respectively, based on the direction.

Bioinformatics Analysis

Online bioinformatics tools microRNA. org(http://www.microrna.org/microrna/get-Downloads.do) and starBase (http: starbase.sysu. edu.cn) were utilized to predict the putative targets of lncRNA and miRNA, respectively.

Dual-Luciferase Reporter Assay

Dual-luciferase reporter assay was conducted to verify the interaction between CASC2 or miR-133b and their targets. Briefly, the wild-type (WT) sequences of CASC2 harboring the binding sites with miR-133b and the mutant (MUT) sequences of CASC2 were amplified and inserted into pmirGLO (Promega, Madison, WI, USA), namely CASC2 WT andCASC2 MUT, respectively. Meanwhile, the WT and MUT sequences of FOXP1 3' UTR were also constructed into pmirGLO, namely FOXP1 3' UTR WT and FOXP1 3' UTR MUT, respectively. Afterwards, HMCs were co-transfected with miR-133b and CASC2 WT, CASC2 MUT, FOXP1 3' UTR WT or FOXP1 3' UTR MUT, and miR-NC was acted as a control. After 48 h, the luciferase activity was examined using the Dual-Luciferase reporter assay system (Promega, Madison, WI, USA).

RNA Pull-Down

RNA pull-down analysis was carried out to further verify the relationship between miR-133b and CASC2 or FOXP1 using RNA-Protein Pull-Down Kit (Thermo Fisher Scientific). In brief, HMCs were transfected with biotinylated miR-133b (Bio-miR-133b-WT), miR-377-3p-MUT (Bio-miR-133b-MUT) and negative control (Bio-miR-NC) (GenePharma, Shanghai, China), respectively. At 48 h after transfection, HMCs were collected and lysed. Afterwards, the cell lysates were incubated with dynabeads streptavidin ac-

cording to the manufacturer's protocol to capture Bio-miR-133b-MUT or Bio-miR-133b-WT compound. After elution with the biotin elution buffer, the complex was used for the measurement of CASC2 level by qRT-PCR analysis.

Statistical Analysis

All experiments were executed at least 3 times. Data was analyzed by GraphPad Prism 5.0 (Version X, La Jolla, CA, USA) and presented as the mean ± standard deviation (SD). For difference comparisons, the Student's *t*-test was used between two groups and one-way analysis of variance followed by Turkey's test was used for comparisons among multiple groups. The Spearman rank correlation coefficient was carried out to determine the correlation between the two parameters. *p*-values less than 0.05 were regarded to be statistically significant.

Results

CASC2 was Down-Regulated, but miR-133b was Up-Regulated in DN

To detect whether CASC2 and miR-133b were aberrantly expressed in DN, the expression of CASC2 and miR-133b was measured. Relative to healthy volunteers (Control, n=50), the expression of CASC2 was reduced in serum of DN patients (n=62) (Figure 1A), while miR-133b was significantly overexpressed in serum of DN patients (Figure 1B). Spearman correlation analysis presented that miR-133b expression was negatively correlated with CASC2 expression (Figure 1C). The data suggested that CASC2 and miR-133b were aberrantly regulated in DN.

CASC2 Upregulation Inhibited HG-Induced HMCs Injury

To determine the potential role of CASC2 in DN, the endogenous level of CASC2 was elevated in HG-induced HMCs. Firstly, we found that the expression of CASC2 in HG-induced HMCs was prominently lower than that in Control (Figure 2A). With the transfection of CASC2, the expression of CASC2 was rapidly increased in HG-induced HMCs (Figure 2B). Next, the CCK-8 assay indicated that the HG-induced proliferation of HMCs was pronouncedly inhibited by CASC2 upregulation (Figure 2C). Besides, the expression of ECM proteins, including Col IV and FN, stimulated by HG, was depleted by CASC2 upregulation at both mRNA and protein levels (Figure 2D and 2E). Moreover, the expression of NOX2 at the protein level induced by HG, was also weakened by CASC2 upregulation (Figure 2F). Additionally, the release of MDA (nmol/mg prot) was promoted by HG but reduced by CASC2 overexpression (Figure 2G), while the release of SOD was opposite to that of the release of MDA (Figure 2H). These data indicated that the injury of HMCs induced by HG was attenuated by CASC2 upregulation.

MiR-133b Was a Target of CASC2

To probe the underlying mechanism of CASC2 in DN, the targets of CASC2 were screened and identified. Database microRNA.org was used to predict the targets of CASC2, and the analysis exhibited that CASC2 had a highly conserved binding site with miR-133b (Figure 3A). Then the dual-luciferase reporter assay was conducted to verify the relationship between SASC2 and miR-133b, and the result showed that the miR-133b transfection significantly reduced the lucif-

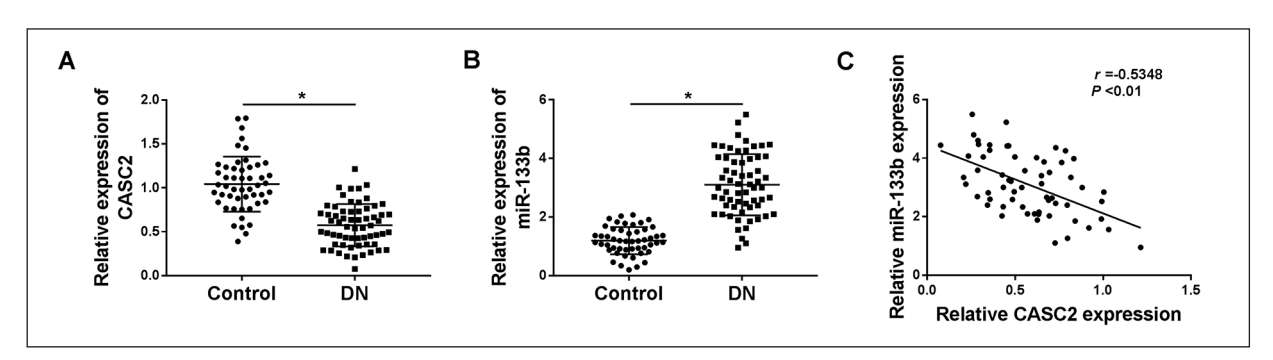


Figure 1. CASC2 was down-regulated in serum from DN patients, but miR-133b was up-regulated. (A) The expression of CASC2 in serum from DN patients and healthy volunteers was measured by qRT-PCR. (B) The expression of miR-133b in serum from DN patients and healthy volunteers. (C) The correlation between miR-133b expression and CASC2 expression was analyzed by the Spearman rank correlation coefficient. *p<0.05.

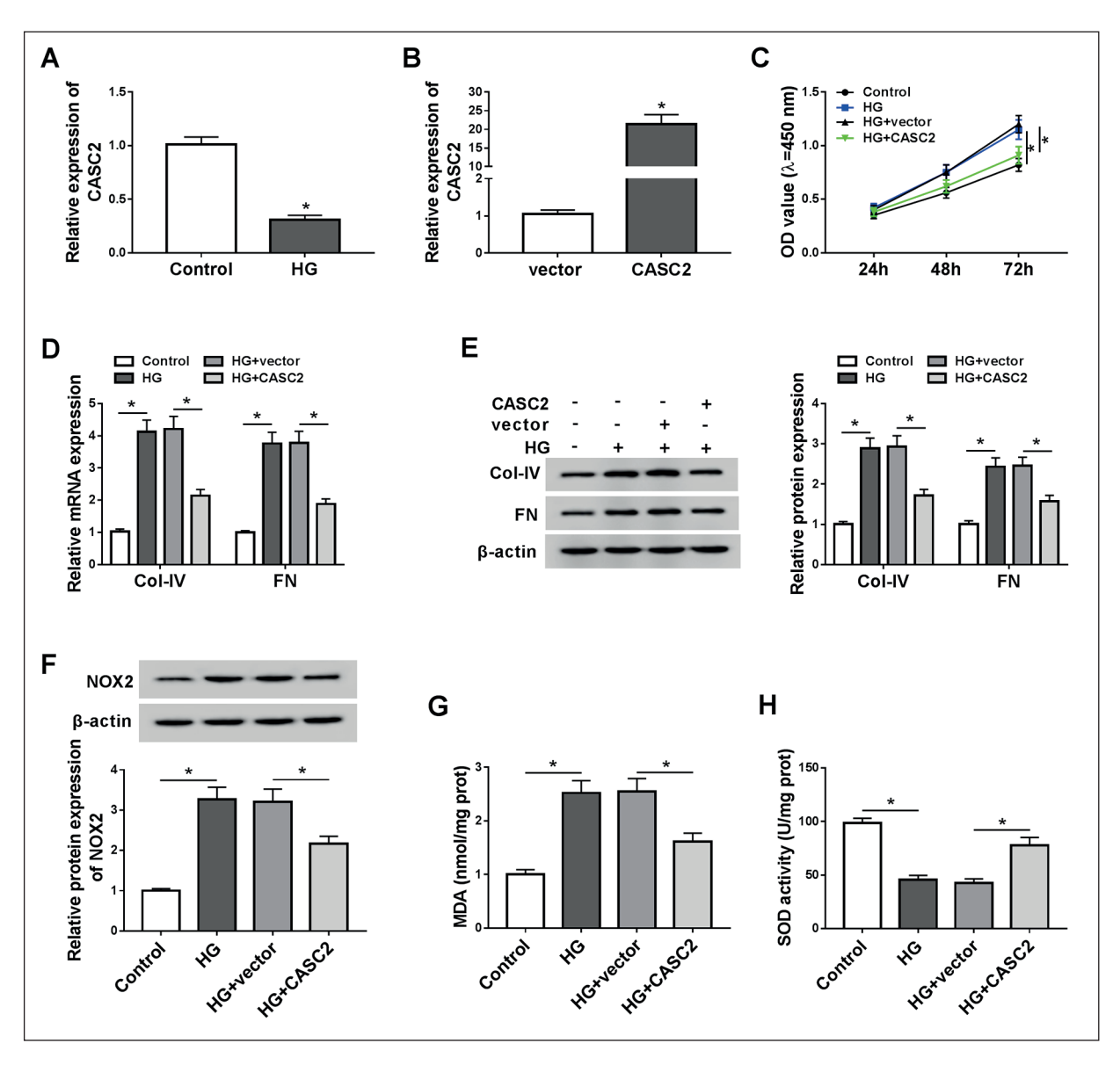


Figure 2. CASC2 upregulation alleviated HG-induced HMCs injury. HMCs treated with or without HG or Control were transfected with CASC2 or vector. (**A**) The expression of CASC2 in HMCs treated with HG or Control. (**B**) The efficiency of CASC2 overexpression. (**C**) Cell proliferation was detected by CCK-8 assay. (**D** and **E**) The expression of Col-IV and FN at mRNA and protein levels was assessed by qRT-PCR and Western blot, respectively. (**F**) The expression of NOX2 at the protein level was quantified by Western blot. (**G** and **H**) The release of MDA and SOD was checked using the corresponding kit. *p<0.05.

erase activity of HMCs transfected with CASC2 WT reporter plasmid, whereas the activity of HMCs transfected with CASC2 MUT reporter plasmid was not affected by miR-133b (Figure 3B). Furthermore, RNA pull-down assay concluded that CASC2 was pronouncedly pulled down by Bio-miR-133b-WT oligos but not the Bio-miR-133b-MUT oligos compared with Bio-miR-NC in HMCs (Figure 3C). Besides, we noticed that the expression of miR-133b was dramatically enhanced in HG-induced HMCs

relative to that in Control (Figure 3D), and the expression of miR-133b was depleted by CASC2 overexpression in HG-induced HMCs (Figure 3E). These data hinted that miR-133b was a direct target of CASC2.

Enrichment of miR-133b Eliminated the Effects of CASC2 Upregulation on HG-Induced HMCs Injury

To examine whether CASC2 affected HMCs injury through regulating miR-133b, miR-133b

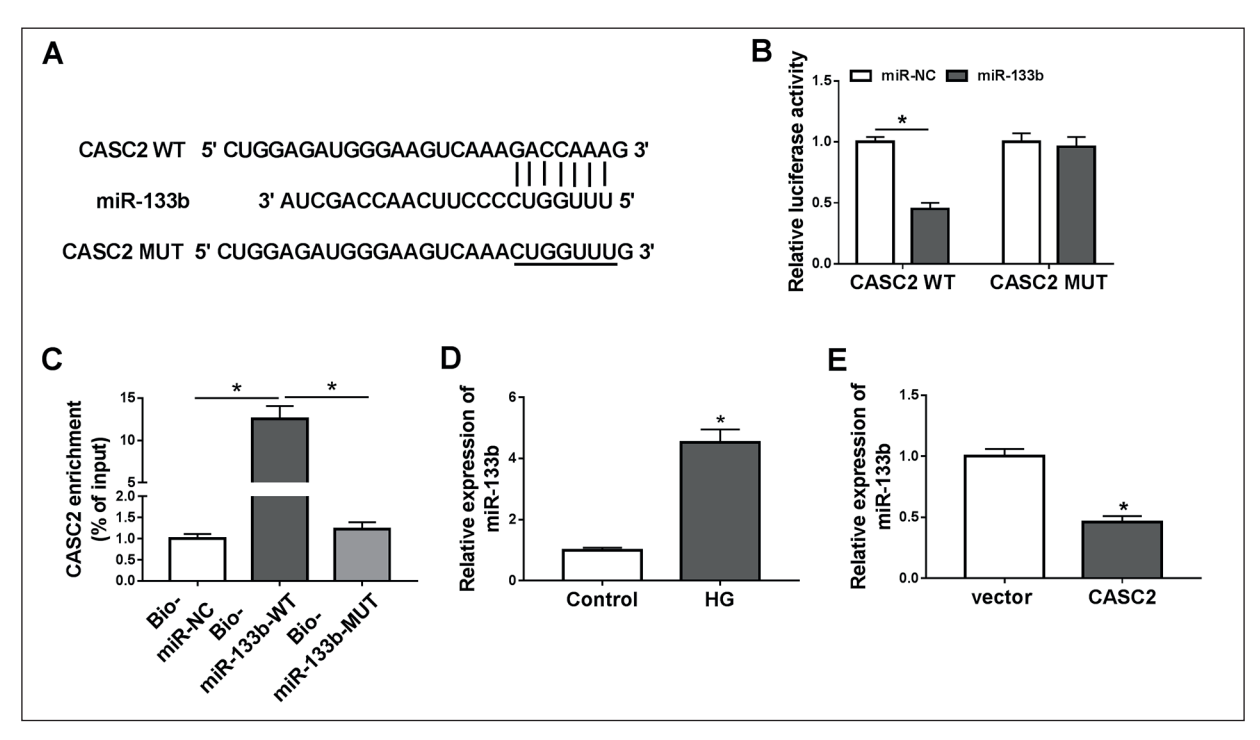


Figure 3. MiR-133b was a target of CASC2. **(A)** The specific binding site between CASC2 and miR-133b was identified by online tool microRNA.org. **(B** and **C)** The relationship between CASC2 and miR-133b was verified by dual-luciferase reporter assay and RNA pull-down. **(D)** The expression of miR-133b in serum from DN patients or healthy volunteers. **(E)** The expression of miR-133b in HMCs transfected with CASC2 or vector. *p < 0.05.

and CASC2+miR-133b were introduced into HG-induced HMCs, respectively, miR-NC and CASC2+miR-NC as the controls. First, the transfection efficiency of miR-133b was tested, and we discovered that the expression of miR-133b was markedly strengthened with the transfection of miR-133b (Figure 4A). The proliferation of HG-induced HMCs transfected with miR-133b was strongly elevated than Control or miR-NC, and miR-133b enrichment reversed the effects of CASC2 upregulation on cell proliferation (Figure 4B). Besides, enrichment of miR-133b intensified the expression of Col IV and FN at both mRNA and protein levels in HG-induced HMCs and restored the levels of Col IV and FN inhibited by CASC2 upregulation (Figure 4C and 4D). Furthermore, the level of NOX2 was promoted by miR-133b enrichment relative to control or miR-NC, and suppressive expression of NOX2 caused by CASC2 upregulation was recovered by miR-133b enrichment (Figure 4E). The release of MDA, blocked by CASC2 upregulation, was increased by miR-133b enrichment (Figure 4F).

On the contrary, miR-133b enrichment could weaken the level of SOD and reduced the level of miR-133b stimulated by CASC2 upregulation

(Figure 4G). All data indicated that enrichment of miR-133b abolished the effects of CASC2 upregulation on HG-induced HMCs injury.

FOXP1 was a Target of miR-133b

To further explore the action mechanism of CASC2 in DN, the downstream targets of miR-133b were screened and verified. There was a specific binding site between miR-133b and FOXP1 3' UTR through online software starBase (Figure 5A). Dual-luciferase reporter assay exhibited that the luciferase activity in HMCs containing miR-133b and FOXP1 3' UTR WT transfection was significantly declined compared with miR-NC but had no noticeable change in HMCs transfected with FOXP1 3' UTR MUT and miR-133b or miR-NC (Figure 5B). Next, we found that the expression of FOXP1 at mRNA and protein levels was notably decreased in HG-induced HMCs relative to Control (Figure 5C and 5D). Besides, the expression of FOXP1 was inhibited by miR-133b enrichment but promoted by miR-133b inhibition at both mRNA and protein levels (Figure 5E and 5F). Moreover, the expression of FOXP1 was elevated in HMCs transfected with CASC2 but depleted in HMCs transfected with CAS-

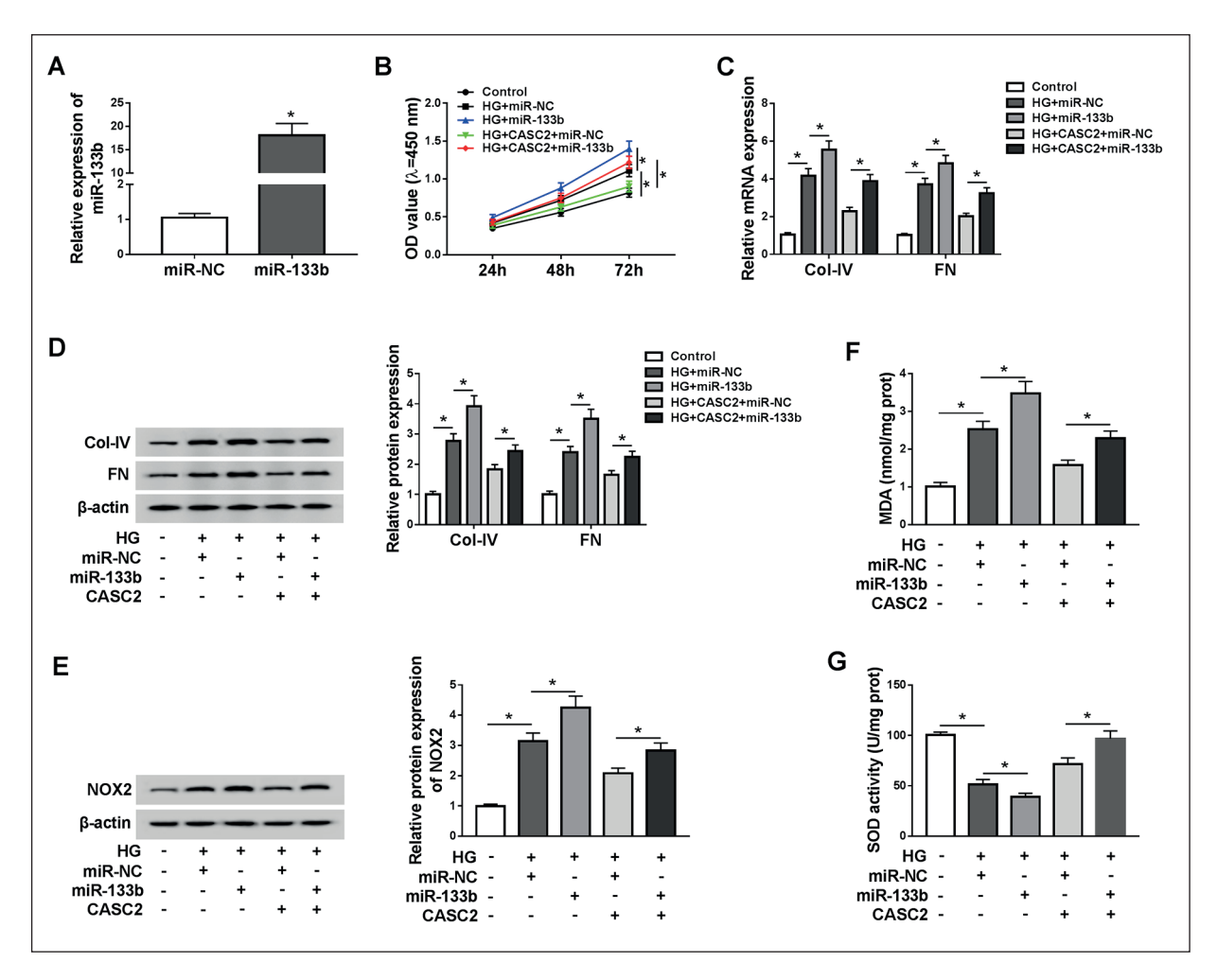


Figure 4. Enrichment of miR-133b abolished the effects of CASC2 upregulation. HMCs treated with HG and Control were introduced with miR-133b, miR-NC, CASC2+miR-133b and CASC2+miR-NC, respectively. (A) The efficiency of miR-133b overexpression. (B) Cell proliferation was assessed by CCK-8 assay. (C and D) The expression of Col-IV and FN at mRNA and protein levels was determined by qRT-PCR and Western blot, respectively. (E) The expression of NOX2 at the protein level was quantified by Western blot. (F and G) The release of MDA and SOD was examined using the corresponding kit. *p<0.05.

C2+miR-133b (Figure 5G and 5H). Summarily, FOXP1 was a target of miR-133b and was regulated by CASC2 through miR-133b.

FOXP1 Knockdown Counteracted the Impact of CASC2 Upregulation in HG-Induced HMCs

To ascertain whether CASC2 exerted its role through the modulation of FOXP1, CASC2, vector, CASC2+si-FOXP1 and CASC2+si-NC were introduced into HG-induced HMCs, respectively. Firstly, the efficiency of FOXP1 interference was checked, and the result showed that the expression of FOXP1 at both mRNA and protein levels in HMCs was sharply reduced with si-FOXP1 transfection compared with si-NC (Figure 6A and

6B). Next, cell proliferation, inhibited by CASC2 upregulation, was recovered by FOXP1 knockdown (Figure 6C). Besides, the expression of Col-IV and FN at both mRNA and protein levels was suppressed in HG-induced HMCs transfected with CASC2 but went up in HG-induced HMCs transfected with CASC2+si-FOXP1 (Figure 6D and 6E). The expression of NOX2 at the protein level was also blocked by CASC2 upregulation but reinforced by FOXP1 knockdown (Figure 6F). Furthermore, the release of MDA was sequestered in cells with CASC2 transfection but enhanced in cells with CASC2+si-FOXP1 transfection (Figure 6G), while the release of SOD was inversely promoted by CASC2 upregulation but declined by FOXP1 knockdown in HG-induced

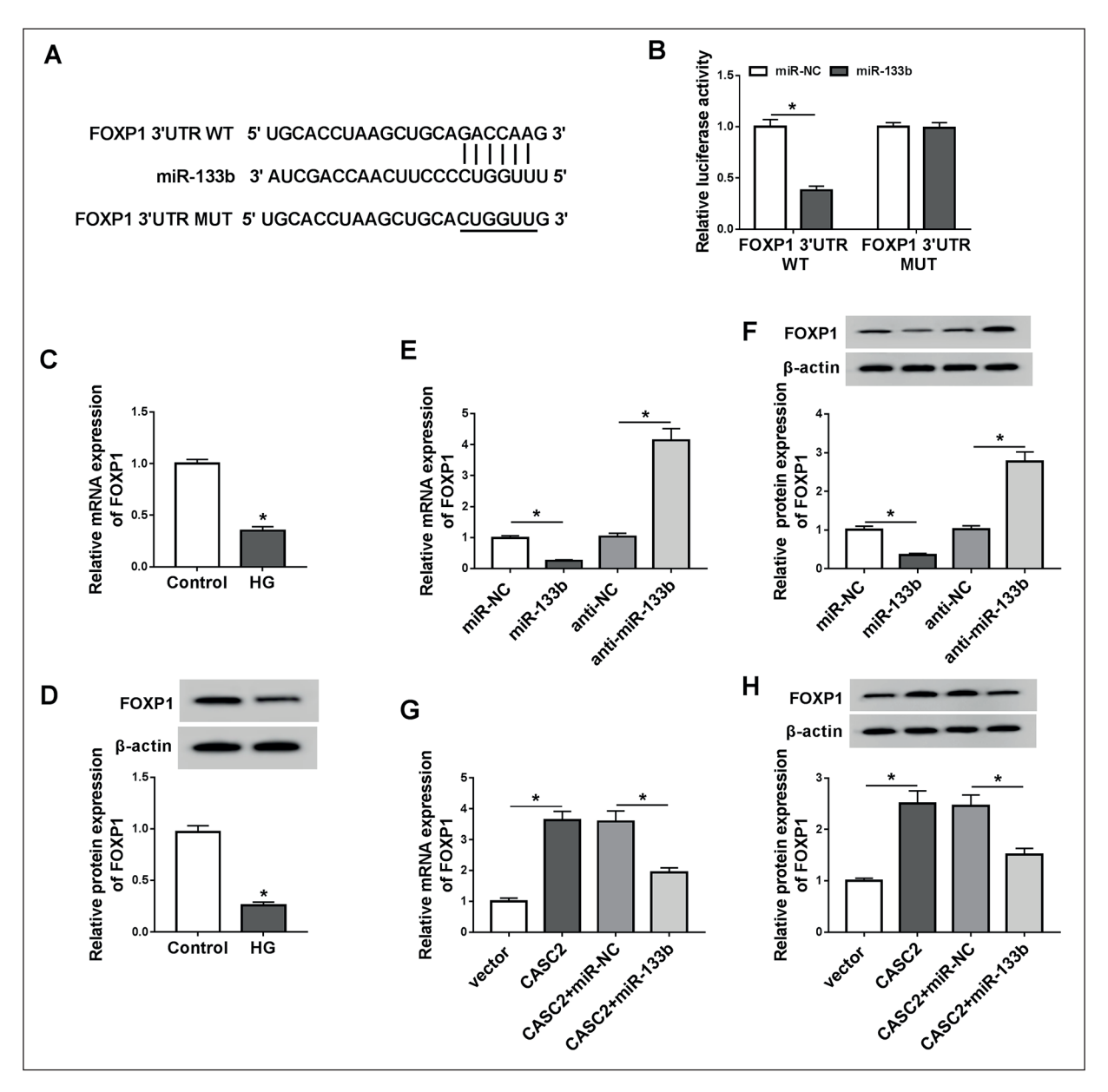


Figure 5. FOXP1 was a target of miR-133b. **(A)** The specific binding site between FOXP1 3' UTR and miR-133b was analyzed by starBase. **(B)** The relationship between FOXP1 and miR-133b was detected by dual-luciferase reporter assay. **(C)** The expression of FOXP1 at the mRNA level in serum from DN patients or healthy volunteers. **(E** and **F)** The expression of FOXP1 at mRNA and protein level in HMCs transfected with miR-133b or anti-miR-133b, miR-NC or anti-NC as the control. **(D)** The expression of FOXP1 at the protein level in HMCs treated with HG or Control. **(G** and **H)** The expression of FOXP1 at mRNA and protein level in HMCs transfected with CASC2 or CASC2+miR-133b, vector or CASC2+miR-NC as the control. *p<0.05.

HMCs (Figure 6H). These analyses summarized that CASC2 upregulation attenuated HG-induced HMCs injury through the increase of FOXP1.

Discussion

DN is a leading complication of diabetes and threatens people's health. In this study, we

found that the expression of CASC2 was aberrantly declined in the serum of DN patients and HG-induced HMCs. Functional analyses revealed that CASC2 upregulation ameliorated HG-induced HMCs injury. Mechanism analyses concluded that miR-133b was a target of CASC2, and FOXP1 was a target of miR-133b. Besides, miR-133b enrichment or FOXP1 knockdown abrogated the effects of CASC2

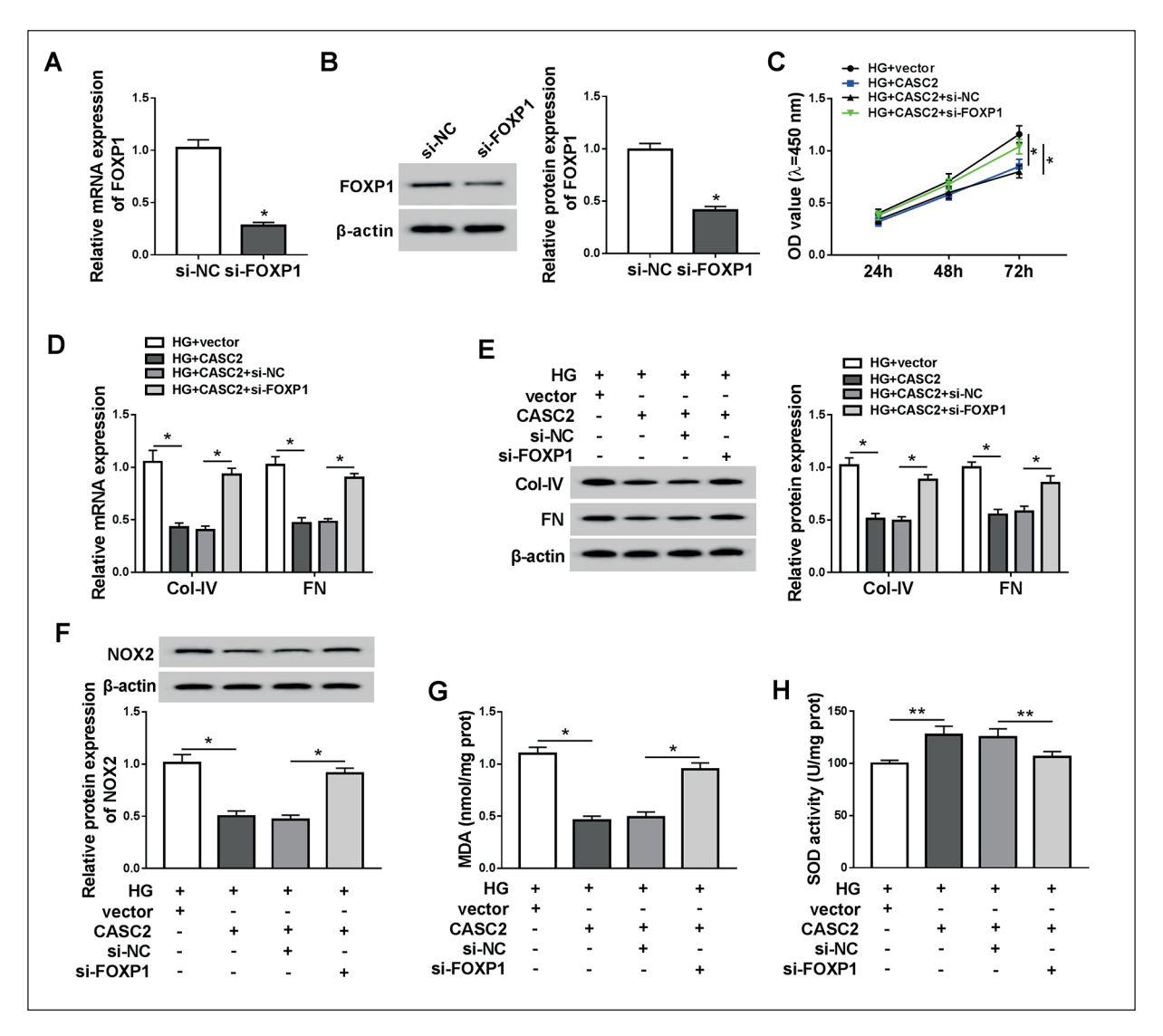


Figure 6. FOXP1 knockdown abrogated the effects of CASC2 upregulation. HMCs treated with HG were transfected with CASC2 or CASC2+si-FOXP1, vector or CASC2+si-NC as the control. (**A** and **B**) The efficiency of FOXP1 knockdown at mRNA and protein levels. (**C**) Cell proliferation was assessed by CCK-8 assay. (**D** and **B**) The expression of Col-IV and FN at mRNA and protein levels was determined by qRT-PCR and Western blot, respectively. (**F**) The expression of NOX2 at the protein level was quantified by Western blot. (**G** and **B**) The release of MDA and SOD was examined using the corresponding kit. *p<0.05.

upregulation. Our study provided a new sight for the understanding of the mechanism in the development of DN.

Typical pathological features of DN include the massive proliferation of mesangial cells, mesangial expansion, hypertrophy and accumulation of ECM proteins (such as collagen and fibronectin) and shedding of podocytes^{29,30}. A previous study showed that CASC2 was down-regulated in serum and renal tissue from type 2 diabetes with renal dysfunction complications¹⁷. Another study discovered that the serum level of CASC2 was notably decreased in DN patients relative to

healthy subjects, and CASC2 overexpression suppressed apoptosis of podocytes³¹. Consistently, our study also elucidated that CASC2 was lowly expressed in the serum of DN patients, as well as in HG-induced HMCs. Moreover, we found that CASC2 upregulation attenuated proliferation, ECM synthesis and oxidative stress of HMCs, indicating that CASC2 overexpression alleviated HG-induced HMCs injury.

It was confirmed that miR-133b was a target of CASC2 through the analyses of the bioinformatics tool, dual-luciferase reporter assay and RNA pull-down. Existing research harbored the idea

that miR-133b was enriched in the renal cortex of diabetic rats and TGF-β1-induced HK-2 cells, and miR-133b inhibition blocked epithelial mesenchymal-transition (EMT) and renal fibrosis³². Eissa et al² showed that miR-133b was richly expressed in type 2 DN patients, and miR-133b could be a novel miRNA panel of DN. In agreement with them, we also determined that the expression of miR-133b was aberrantly enhanced in the serum of DN patients and HG-induced HMCs. Besides, miR-133b enrichment reversed the regulatory effects of CASC2 upregulation in HG-induced HMCs, leading to the reacquisition of HG-induced HMCs injury.

FOXP1 was confirmed as a downstream target of miR-133b. A previous study alleged that the expression level of FOXP1 was remarkably depleted in MCs induced by HG, and overexpression of FOXP1 inhibited HG-induced cell proliferation, the expression of ECM proteins and oxidative stress through the modulation of AKT/mTOR pathway ²⁸. Similar results were observed in our investigation, suggesting that FOXP1 contributed to the inhibition of HG-induced HMCs injury.

Conclusions

Taken together, the above results demonstrated that CASC2 was down-regulated in the serum of DN patients and HG-induced HMCs, and its upregulation blocked HG-induced HMCs proliferation, ECM accumulation and oxidative stress. Furthermore, our study firstly revealed that CASC2 exerted its role in HG-induced HMCs though the miR-133b/FOXP1 axis, supplying a novel mechanism of DN development and a promising biomarker for the therapeutic strategy of DN.

Conflict of Interest

The Authors declare that they have no conflict of interests.

References

- 1) Rubino F. Medical research: time to think differently about diabetes. Nature 2016; 533: 459-461.
- EISSA S, MATBOLI M, BEKHET MM. Clinical verification of a novel urinary microRNA panal: 133b, -342 and -30 as biomarkers for diabetic nephropathy identified by bioinformatics analysis. Biomed Pharmacother 2016; 83: 92-99.

- Lei L, Mao Y, Meng D, Zhang X, Cui L, Huo Y, Wang Y. Percentage of circulating CD8+ T lymphocytes is associated with albuminuria in type 2 diabetes mellitus. Exp Clin Endocrinol Diabetes 2014; 122: 27-30.
- ARORA MK, SINGH UK. Molecular mechanisms in the pathogenesis of diabetic nephropathy: an update. Vascul Pharmacol 2013; 58: 259-271.
- MIMA A. Inflammation and oxidative stress in diabetic nephropathy: new insights on its inhibition as new therapeutic targets. J Diabetes Res 2013; 2013: 248563.
- CATHERWOOD MA, POWELL LA, ANDERSON P, McMaster D, SHARPE PC, TRIMBLE ER. Glucose-induced oxidative stress in mesangial cells. Kidney Int 2002; 61: 599-608.
- FLYNN C, BAKRIS GL. Noninsulin glucose-lowering agents for the treatment of patients on dialysis. Nat Rev Nephrol 2013; 9: 147-153.
- 8) FRIED LF, EMANUELE N, ZHANG JH, BROPHY M, CONNER TA, DUCKWORTH W, LEEHEY DJ, McCULLOUGH PA, O'CONNOR T, PALEVSKY PM, REILLY RF, SELIGER SL, WARREN SR, WATNICK S, PEDUZZI P, GUARINO P; VA NEPHRON-D Investigators. Combined angiotensin inhibition for the treatment of diabetic nephropathy. N Engl J Med 2013; 369: 1892-1903.
- ALVAREZ ML, KHOSROHEIDARI M, EDDY E, KIEFER J. Role of microRNA 1207-5P and its host gene, the long non-coding RNA Pvt1, as mediators of extracellular matrix accumulation in the kidney: implications for diabetic nephropathy. PLoS One 2013; 8: e77468.
- ALVAREZ ML, DISTEFANO JK. Functional characterization of the plasmacytoma variant translocation 1 gene (PVT1) in diabetic nephropathy. PLoS One 2011; 6: e18671.
- 11) ZHUANG YT, XU DY, WANG GY, SUN JL, HUANG Y, WANG SZ. IL-6 induced IncRNA MALAT1 enhances TNF-alpha expression in LPS-induced septic cardiomyocytes via activation of SAA3. Eur Rev Med Pharmacol Sci 2017; 21: 302-309.
- 12) LONG J, BADAL SS, YE Z, WANG Y, AYANGA BA, GALVAN DL, GREEN NH, CHANG BH, OVERBEEK PA, DANESH FR. Long noncoding RNA Tug1 regulates mitochondrial bioenergetics in diabetic nephropathy. J Clin Invest 2016; 126: 4205-4218.
- 13) DUAN LJ, DING M, HOU LJ, CUI YT, LI CJ, YU DM. Long noncoding RNA TUG1 alleviates extracellular matrix accumulation via mediating microR-NA-377 targeting of PPARgamma in diabetic nephropathy. Biochem Biophys Res Commun 2017; 484: 598-604.
- 14) Sun J, Liu L, Zou H, Yu W. The long non-coding RNA CASC2 suppresses cell viability, migration, and invasion in hepatocellular carcinoma cells by directly downregulating miR-183. Yonsei Med J 2019; 60: 905-913.
- 15) ZHENG P, DONG L, ZHANG B, DAI J, ZHANG Y, WANG Y, QIN S. Long noncoding RNA CASC2 promotes paclitaxel resistance in breast cancer through regulation of miR-18a-5p/CDK19. Histochem Cell Biol 2019; 152: 281-291.

- 16) DAI W, Mu L, CUI Y, LI Y, CHEN P, XIE H, WANG X. Long noncoding RNA CASC2 enhances berberineinduced cytotoxicity in colorectal cancer cells by silencing BCL2. Mol Med Rep 2019; 20: 995-1006.
- 17) Wang L, Su N, Zhang Y, Wang G. Clinical significance of serum IncRNA cancer susceptibility candidate 2 (CASC2) for chronic renal failure in patients with type 2 diabetes. Med Sci Monit 2018; 24: 6079-6084.
- Acunzo M, Croce CM. MicroRNA in cancer and cachexia--a mini-review. J Infect Dis 2015; 212: S74-S77.
- 19) BARUTTA F, TRICARICO M, CORBELLI A, ANNARATONE L, PINACH S, GRIMALDI S, BRUNO G, CIMINO D, TAVERNA D, DEREGIBUS MC, RASTALDI MP, PERIN PC, GRUDEN G. Urinary exosomal microRNAs in incipient diabetic nephropathy. PLoS One 2013; 8: e73798.
- 20) WANG LP, GAO YZ, SONG B, YU G, CHEN H, ZHANG ZW, YAN CF, PAN YL, YU XY. MicroRNAs in the progress of diabetic nephropathy: a systematic review and meta-analysis. Evid Based Complement Alternat Med 2019; 2019: 3513179.
- YANG Q, ZHAO Q, YIN Y. miR-133b is a potential diagnostic biomarker for Alzheimer's disease and has a neuroprotective role. Exp Ther Med 2019; 18: 2711-2718.
- 22) MASE M, GRASSO M, AVOGARO L, NICOLUSSI GIACOM-AZ M, D'AMATO E, TESSAROLO F, GRAFFIGNA A, DENTI MA, RAVELLI F. Upregulation of miR-133b and miR-328 in patients with atrial dilatation: implications for stretch-induced atrial fibrillation. Front Physiol 2019; 10: 1133.
- 23) Lv L, Li Q, Chen S, Zhang X, Tao X, Tang X, Wang S, Che G, Yu Y, He L. miR-133b suppresses colorec-

- tal cancer cell stemness and chemoresistance by targeting methyltransferase DOT1L. Exp Cell Res 2019; 385: 111597.
- 24) BUSHATI N, COHEN SM. microRNA functions. Annu Rev Cell Dev Biol 2007; 23: 175-205.
- 25) Zou Y, Gong N, Cui Y, Wang X, Cui A, Chen Q, Jiao T, Dong X, Yang H, Zhang S, Fang F, Chang Y. Forkhead Box P1 (FOXP1) transcription factor regulates hepatic glucose homeostasis. J Biol Chem 2015; 290: 30607-30615.
- 26) Kanter JE. FOXP1: a gatekeeper of endothelial cell inflammation. Circ Res 2019; 125: 606-608.
- SHENG H, Li X, Xu Y. Knockdown of FOXP1 promotes the development of lung adenocarcinoma. Cancer Biol Ther 2019; 20: 537-545.
- 28) XIANG H, XUE W, WU X, ZHENG J, DING C, LI Y, DOU M. FOXP1 inhibits high glucose-induced ECM accumulation and oxidative stress in mesangial cells. Chem Biol Interact 2019; 313: 108818.
- CAO Z, COOPER ME. Pathogenesis of diabetic nephropathy. J Diabetes Investig 2011; 2: 243-247.
- KANWAR YS, SUN L, XIE P, LIU FY, CHEN S. A glimpse of various pathogenetic mechanisms of diabetic nephropathy. Annu Rev Pathol 2011; 6: 395-423.
- 31) YANG H, KAN QE, Su Y, MAN H. Long non-coding RNA CASC2 improves diabetic nephropathy by inhibiting JNK pathway. Exp Clin Endocrinol Diabetes 2019; 127: 533-537.
- 32) SUN Z, MA Y, CHEN F, WANG S, CHEN B, SHI J. miR-133b and miR-199b knockdown attenuate TGF-beta1-induced epithelial to mesenchymal transition and renal fibrosis by targeting SIRT1 in diabetic nephropathy. Eur J Pharmacol 2018; 837: 96-104.